



Published in final edited form as:

J Med Genet. ; 61(4): 369–377. doi:10.1136/jmg-2023-109473.

Titin copy number variations associated with dominant inherited phenotypes

Aurélien Perrin^{1,2}, Corinne Métay^{3,4}, Marco Savarese⁵, Rabah Ben Yaou⁴, German Demidov⁶, Isabelle Nelson⁴, Guilhem Solé⁷, Yann Péréon⁸, Enrico Silvio Bertini⁹, Fabiana Fattori⁹, Adele D'Amico⁹, Federica Ricci¹⁰, Mira Ginsberg¹¹, Andreea Seferian¹², Odile Boespflug-Tanguy^{12,13}, Laurent Servais^{12,14,15}, Françoise Chapon¹⁶, Emmeline Lagrange¹⁷, Karen Gaudon³, Adrien Bloch³, Robin Ghanem³, Lucie Guyant-Maréchal¹⁸, Mridul Johari^{5,19}, Charles Van Goethem^{1,20}, Michel Fardeau⁴, Raul Juntas Morales²¹, Casie A Genetti²², Minttu Marttila^{22,23}, Michel Koenig^{1,2}, Alan H Beggs²², Bjarne Udd⁵, Gisèle Bonne⁴, Mireille Cossée^{1,2}

¹Laboratoire de Génétique Moléculaire, Centre Hospitalier Universitaire de Montpellier, Montpellier, France

²PhyMedExp, Université de Montpellier, INSERM, CNRS, Montpellier, France

³Unité Fonctionnelle de Cardiogénétique et Myogénétique moléculaire et cellulaire, Centre de Génétique Moléculaire et Chromosomique, Groupe Hospitalier La Pitié-Salpêtrière-Charles Foix, Paris, France

⁴Sorbonne Université, INSERM, Institut de Myologie, Centre de Recherche en Myologie, Paris, France

⁵Tampere Neuromuscular Center, Folkhälsan Research Center, Helsinki, Finland

⁶Institute of Medical Genetics and Applied Genomics, University of Tübingen, Tübingen, Germany

⁷CHU de Bordeaux, AOC National Reference Center for Neuromuscular Disorders, Bordeaux, France

Correspondence to Dr Mireille Cossée and Dr Aurélien Perrin, Laboratoire de Génétique Moléculaire, Centre Hospitalier Universitaire de Montpellier, 34093 Montpellier, France; mireille.cossee@inserm.fr, aurelien.perrin@ext.inserm.fr.

Contributors AP, CM, MS, AB, BU, GB and MC contributed to the conception and design of the study. All authors contributed to the acquisition and analysis of data. AP, CM, MS, RBY, CVG, BU and MC contributed to drafting a significant portion of the manuscript or figures. MC and AP are the guarantors of this study. AP and MC contributed equally.

Additional supplemental material is published online only. To view, please visit the journal online (<http://dx.doi.org/10.1136/jmg-2023-109473>).

Competing interests None declared.

Patient consent for publication Obtained.

Ethics approval The study was approved by the ethical guidelines issued by our institutions for clinical studies in compliance with the Helsinki Declaration. Patients gave informed consent for the genetic analysis according to the French legislation (Comité de Protection des Personnes OUEST 6-CPP1128HPS3 IDRCB-2018-AO2287-48).

Supplemental material This content has been supplied by the author(s). It has not been vetted by BMJ Publishing Group Limited (BMJ) and may not have been peer-reviewed. Any opinions or recommendations discussed are solely those of the author(s) and are not endorsed by BMJ. BMJ disclaims all liability and responsibility arising from any reliance placed on the content. Where the content includes any translated material, BMJ does not warrant the accuracy and reliability of the translations (including but not limited to local regulations, clinical guidelines, terminology, drug names and drug dosages), and is not responsible for any error and/or omissions arising from translation and adaptation or otherwise.

⁸Department of Clinical Neurophysiology, Reference Centre for Neuromuscular Diseases AOC, Filnemus, Euro-NMD, CHU Nantes, Nantes Université, Place Alexis-Ricordeau, Nantes, France

⁹Unit of Muscular and Neurodegenerative Disorders, Bambino Gesù Children Research Hospital, IRCCS, Rome, Italy

¹⁰Division of Child and Adolescent Neuropsychiatry, University of Turin, Turin, Italy

¹¹Department of Pediatric Neurology, Wolfson Medical Center, Holon, Israel

¹²Institut I-MOTION, Hôpital Armand Trousseau, Paris, France

¹³UMR 1141, INSERM, NeuroDiderot Université Paris Cité and APHP, Neuropédiatrie, French Reference Center for Leukodystrophies, LEUKOFRANCE, Hôpital Robert Debré, Paris, France

¹⁴MDUK Oxford Neuromuscular Centre & NIHR Oxford Biomedical Research Centre, University of Oxford, Oxford, UK

¹⁵Neuromuscular Reference Center, Division of Paediatrics, University and Hospital University of Liège, Liège, Belgium

¹⁶Département de pathologie, Centre de Compétence des Maladies Neuromusculaires, Centre Hospitalier Universitaire de Caen, Caen, France

¹⁷Centre de Compétences des Maladies Neuro Musculaires, Centre Hospitalier Universitaire Grenoble Alpes, Grenoble, France

¹⁸Department of Neurophysiology, Rouen University Hospital, Rouen, France

¹⁹Harry Perkins Institute of Medical Research, Centre for Medical Research, University of Western Australia, Nedlands, Western Australia, Australia

²⁰Montpellier BioInformatique pour le Diagnostic Clinique (MOBIDIC), Plateau de Médecine Moléculaire et Génomique (PMMG), CHU Montpellier, Montpellier, France

²¹Department of Neurology, Hospital Universitario Vall d'Hebron, Universitat Autònoma de Barcelona, Barcelona, Spain

²²Division of Genetics and Genomics, The Manton Center for Orphan Disease Research, Boston Children's Hospital, Harvard Medical School, Boston, Massachusetts, USA

²³HiLIFE Helsinki Institute of Life Science, Tukholmankatu 8, FI-00014, University of Helsinki, Helsinki, Finland

Abstract

Background—Titinopathies are caused by mutations in the titin gene (*TTN*). Titin is the largest known human protein; its gene has the longest coding phase with 364 exons. Titinopathies are very complex neuromuscular pathologies due to the variable age of onset of symptoms, the great diversity of pathological and muscular impairment patterns (cardiac, skeletal muscle or mixed) and both autosomal dominant and recessive modes of transmission. Until now, only few CNVs in *TTN* have been reported without clear genotype–phenotype associations.

Methods—Our study includes eight families with dominant titinopathies. We performed next-generation sequencing or comparative genomic hybridisation array analyses and found CNVs

in the *TTN* gene. We characterised these CNVs by RNA sequencing (RNAseq) analyses in six patients' muscles and performed genotype–phenotype inheritance association study by combining the clinical and biological data of these eight families.

Results—Seven deletion-type CNVs in the *TTN* gene were identified among these families. Genotype and RNAseq results showed that five deletions do not alter the reading frame and one is out-of-reading frame. The main phenotype identified was distal myopathy associated with contractures. The analysis of morphological, clinical and genetic data and imaging let us draw new genotype–phenotype associations of titinopathies.

Conclusion—Identifying *TTN* CNVs will further increase diagnostic sensitivity in these complex neuromuscular pathologies. Our cohort of patients enabled us to identify new deletion-type CNVs in the *TTN* gene, with unexpected autosomal dominant transmission. This is valuable in establishing new genotype–phenotype associations of titinopathies, mainly distal myopathy in most of the patients.

INTRODUCTION

Titinopathies are caused by mutations in the titin (*TTN*) gene. Titin is the largest human protein (3800 kDa); its gene has the largest known coding phase with 364 exons.¹ Titinopathies are complex neuromuscular pathologies for several reasons: age at onset is variable, there is great diversity of phenotypes with various muscular impairments (cardiac, skeletal muscle or mixed impairments) and both autosomal dominant and recessive transmission modes are possible.² Other reasons, notably limited understanding of the pathophysiological mechanisms, limit the interpretation of *TTN* variants and confirmation of the cause of muscle pathology. The size of the gene, titin interactions with other proteins as well as the development of more sensitive sequencing and *TTN* variant analytical technologies are improving our understanding of the diversity of described phenotypes and leading to delineation of new phenotypes associated with *TTN* variants.³

So far, few *TTN* CNVs have been reported. One published *TTN* CNV is a recessive large deletion of exons 34–41, associated in trans with a frameshift mutation p.(Lys3596Asnfs*), reported in a family with a severe phenotype (loss of ambulation before the age of 40 years and marked hyperCKemia). Roggenbuck *et al*^{4,5} described a deletion of exons 346–362 (A-band) predicted to cause a frameshift with early-onset skeletal muscle involvement and dilated cardiomyopathy (DCM) developing in later life.⁵ We previously reported a dominant deletion of *TTN* exons 11–18 resulting in a 16 nucleotide long intron retention between exons 10 and 19 in skeletal muscle transcripts, in two families with a distal titinopathy.⁶ The standard method for CNV detection is comparative genomic hybridisation (CGH) array,⁷ although the short size of the oligoprobes and the repetitive structure of *TTN* are possible limitations to be considered. Recently, several studies have shown that next-generation sequencing (NGS) combined with the use of powerful bioinformatics methods improves the CNV detection.^{4,8} Small CNVs, in particular single-exon deletions and duplication, are still difficult to detect and *TTN* triplicate region is particularly challenging.^{4,8} Despite the aforementioned technical challenges, we present in this study 17 patients from 8 families with dominant CNV in the *TTN* gene, identified by NGS or CGH array.

MATERIALS AND METHODS

Genetic analysis, bioinformatics analysis and variant interpretation

For probands from families A, C, D and E, gDNAs (extracted from blood samples) were used for custom-targeted gene enrichment and DNA library preparation was performed using Nimblegen EZ choice probes and Kappa HTP Library preparation kits according to the manufacturer's instructions (Nimblegen, Roche Diagnostics, Madison, Wisconsin, USA). Paired-end sequencing was performed using the Illumina MiSeq platform (Illumina, Santa Cruz, California, USA). NGS data were analysed using in-house pipelines for detection of single nucleotide variants and CNVs. Detection of CNVs was performed after coverage normalisation by computing the ratio of a target's coverage of a given individual over the mean coverage of this target across all patients of the same sequencing run.⁹

For family B, as part of the Myocapture Project, whole-exome sequencing (WES) was performed by the Centre National de Recherche en Génomique Humaine, Evry, France on DNA samples from patients II-1, II-2, III-1 and IV-3. Variants were annotated and filtered using an in-house software system (PolyWeb). The CNV analysis was performed within the Solve-RD (<https://solve-rd.eu/>) Project after uploading fastq files in RD-Connect (<https://rd-connect.eu/>).

Trio analysis of family F used CGH array and Myocap V.6 (targeted panel covering *TTN* exons and introns).¹⁰

In family G, a CGH array, using the platform SurePrint G3 60K platform (Agilent, California, USA), was performed on the proband and his parents. Proband's DNA was also analysed by Myocap V.6.

In family H (local ID BOS1210), the *TTN* deletion was initially identified by read depth analysis on a next-generation 43-gene sequencing panel as described.¹¹ Trio WES was also performed at the Broad Institute of MIT and Harvard and analysed via the Boston Children's Hospital Rare Disease Cohorts (CRDC) Project, as described previously.¹² Long-range whole-genome sequencing was performed on a PacBio, Sequel II platform at GeneDx (Gaithersburg, Maryland, USA).

CNV confirmation on proband's DNA and variant familial segregation analyses were performed by targeted Sanger sequencing, qPCR or digital droplet PCR (ddPCR).

Transcript analyses

mRNAs were extracted from muscle biopsies and prepared as described in Zenagui *et al*⁹ or using Qiagen RNeasy Plus Universal Mini Kit (Qiagen, Hilden, Germany).

RNA sequencing (RNAseq) analyses were performed as described in Perrin *et al*.¹³ For families F and H, RNAseq was performed by Novogene (Durham, North Carolina, USA) using an Illumina Ribo-Zero Gold kit for ribodepletion followed by NEBNext Ultra II Stranded Library Prep Kit and sequenced to 100 M 2×150 bp paired-end reads. Data processing was performed by the CRDC¹² for family H and Illumina NovaSeq6000

for family F. RNA sequence alignments for all datasets were performed using splice-aware RNAseq aligner (STAR) software¹⁴ and analysed using Integrative Genomics Viewer¹⁵ targeted on titin transcripts, NM_001267550.2 and represent as sashimi plot with ggsashimi algorithm.¹⁶ For the sequence variant nomenclature, we followed the Human Genome Variation Society recommendations and used the *TTN* transcript reference NM_001267550.2, and sequence alignment against the human reference genome (Hg19) was performed.

RESULTS

Clinical data

Pedigrees of all families are represented in figure 1. Main clinical, histological and imaging data are summarised in online supplemental table 1.

Family A is characterised by four affected members, all males, in two generations. The proband (II-3) was referred for distal myopathy of inferior limbs since teenage years. The evolution of muscular damages was gradual and it was associated with cardiomyopathy (arrhythmias on ECG atrial hyperexcitability). Presenting symptoms included pes cavus, running difficulties and steppage gait. Muscle CT scan was normal in the upper limbs, but showed bilateral and symmetrical atrophy of the rectus abdominis, semitendinosus, triceps sural and extensor digitorum of the toes. Electromyography (EMG) revealed a myogenic pattern in the tibialis anterior (60 years old). Muscle biopsy performed at early 60s in the tibialis anterior was normal and electron microscopy showed abnormalities of Z-discs and presence of elongated non-quadrilateral structures extending along the sarcomeres evoking pseudo-rods. His brother (II-2) presented with distal myopathy, pes cavus, head drooping but no limitation in walking. Symptoms started in the teenage years with pes cavus, claw toes and steppage gait. Muscle CT scan (early 60s) showed no abnormality in the upper limbs, but fatty atrophy of the lower limbs and paravertebral muscles were observed. Muscle biopsy was not performed. No cardiac abnormality was noticed (echography and effort test in early 60s). Their brother (II-1) had myopathy and sudden death in late 50s. Their deceased father exhibited camptocormia and cardiac features. No genetic analysis was performed for these two family members.

Family B includes two affected subjects, a father (II-1) and his son (III-3). Patient II-1 acquired walking late (after 18 months) and immediately with tiptoeing. Overt climbing stairs difficulties appeared at 3–4 years of age. The disease evolved with predominant distal weakness and progression to loss of ambulation at the end of adolescence. Muscle CT scan assessment during the late third decade of life (no image available) revealed pelvifemoral involvement in addition to selective involvement of tibialis anterior muscles. In late 40s, a clinically prominent distal involvement in the four limbs was evident. More recent assessments during the fifth and sixth decades of life revealed a more diffuse muscle pattern of weakness and wasting in the four limbs as well as axial muscles (figure 2). Additional features observed at these late stages included joint contractures (hips, knees, Achilles tendons), wrist and finger hyperlaxity and facial weakness. Creatine kinase (CK) was moderately elevated in the young ages. Cardiac assessment was normal throughout disease progression. Conversely, respiratory function was altered in late 20s, requiring

nocturnal non-invasive ventilation from late 30s and became permanent after 50 years old. Muscle biopsy performed after 30 years (deltoid muscle) showed a mild fibre atrophy, type 1 fibre semiuniformity with core-like intermyo-fibrillar network abnormalities.

In patient III-3, the onset of the disease occurred during childhood when parents observed clumsy walking and running and fatigability. At the first assessment at the end of adolescence, there was a predominant distal muscle weakness in the four limbs associated with hamstring contractures, wrist/finger hyperlaxity and facial weakness, although muscle CT scan revealed only mild gluteus maximus muscle fatty infiltration. Muscle biopsy, done at the end of adolescence, showed non-specific findings including fibre size variation, increased number of internalised nuclei and type 1 fibre predominance. However, immunofluorescence studies showed reduced and irregular dystrophin (Dys1 and Dys3 antibodies) and dysferlin stainings. Muscle western blot analysis revealed normal dystrophin amounts with very slightly reduced molecular weight. At that time, a hypothesis was raised that III-1 and his father (II-1) had two different diseases: III-1 possibly having dystrophinopathy and II-1 a myopathy with core-like abnormalities. Patient III-1's exome analysis through Myocapture and Solve-RD Projects did not show any *DMD* or other sarcoglycans and dysferlin gene pathogenic variants. Furthermore, *DMD* gene mRNA did not show any mutation thus definitely infirming the dystrophinopathy hypothesis in III-1 patient and suggesting that dystrophin abnormalities were probably secondary to an unidentified alteration. Motor difficulties evolved progressively, the patient being unable to climb stairs and having difficulties to get up from the chair at the end of 20s. In early 30s, muscle weakness was more diffuse but still predominating in the distal parts of the four limbs. Conversely, to his father who lost walking at the end of adolescence, the disease course seemed less incapacitating as he is still walking at 30 years old, although with frequent falls. Cardiac assessment at 17 years revealed DCM. Last assessment in early 30s confirmed the DCM which responded favourably to perindopril and bisoprolol treatments. Respiratory function at age 30 years was moderately decreased (vital capacity 2.75 L, 58%) not requiring any respiratory support.

Family C includes three affected subjects with variable disease course and severity.

In the mother (I-1), extensive but mild joint contractures were observed since young adult age, but no muscle weakness was observed. The older affected son (II-1) developed ankle joint contractures during childhood. Last assessment in early 10s revealed mild lower limb proximal weakness after prolonged walking or exercise. Joint contractures affected mainly ankles and mildly shoulders and hips. A moderately elevated CK (five times the normal upper value) was noticed during childhood. Muscle imaging was normal during this period. Cardiac assessments in the mother and the eldest son were normal. The younger affected son (II-3) showed delayed motor milestones. When assessed at before 3 years old, the phenotype was considered consistent with type 2 spinal muscular atrophy (SMA-II) with preserved distal motor functions and the presence of knee contractures. A biallelic *SMN1* gene exon 7 homozygous deletion was found and the patient was treated with nusinersen. The disease course was characterised by unusual diffuse joint contractures (elbows, wrists, fingers, ankles) that appeared after 6 years of age.

No *SMNI* gene deletion was found in the oldest affected brother thus suggesting that *SMNI* gene deletion does not explain the disease in the oldest brother or the mother.

Family D reported previously⁶ includes four affected female patients in two generations, with an adult age of onset (40–52 years old) and asymmetric distal myopathy. Patient II-1 and her mother (I-2) are more severely affected than II-2 and II-3 who had a mild right anterior lower leg muscle atrophy.

In family E already reported,⁶ patient III-1 developed difficulty walking and, in early 50s, developed difficulty climbing stairs. Symptoms progressed after 65 years old with the use of a cane, and in early 70s, he had weakness in the right upper limb, frequent falling and used a wheelchair soon after. The last neurological examination, in early 80s, showed considerable proximal (in the posterior thighs) and distal muscle atrophy in both lower and upper limbs and comparable proximodistal weakness. The daughter (patient IV-1) evaluated at mid-50s, initially reported as asymptomatic, presented with discrete clinical abnormalities: anterior distal leg weakness predominantly on the right and childhood Achilles tendon contracture (has never been able to squat with feet on the ground) with hammer toe retraction, predominantly on the right.

Family F is a sporadic case. Currently, the proband is a child, born after uneventful pregnancy and labour to non-consanguineous parents. In the first months of life, asymptomatic non-compaction cardiomyopathy was diagnosed. Since the age of 3 years, she exhibited impaired motor skills, frequent falls and progressive muscle weakness of proximal and distal muscles, mostly of the lower limbs. In addition, there were some facial dysmorphic features, mild microcephaly and learning difficulties. Her gait was asymmetric with left tendon Achilles contraction that required surgical correction. Serum CK levels were normal. EMG demonstrated mild myopathic features. She complains of fatigability, exercise intolerance and myalgia. Muscle MRI showed only minor fat replacement changes of the left calf muscles, with smaller volume than in the right calf, and with severe contracture. Degenerative muscle tissue changes are present in the tibialis anterior muscles, more on the right side and in the left semimembranosus.

Family G includes a sporadic severely affected patient, with congenital arthrogryposis and weakness and delayed motor development during childhood. Family history is negative for neurological disorders. He was a full-term first born, with transient hyperbilirubinaemia after an uneventful pregnancy with scheduled CT for breech presentation, with birth weight 2.890 kg at 39 weeks' gestation. At birth, upper limbs were flexed and leaning against the trunk. Supplemental O₂ was provided for the first 2 days of life because of respiratory distress and some swallowing disturbances. On the third day, transitory hyperCKemia was found up to 1187 IU/L. The child had arthrogryposis with flexed elbows, bilateral camptodactyly of the fifth finger and contractures of his left foot. At age 1 month, worsening respiratory function with hypercapnia led to temporary O₂ therapy and a nasogastric (NG) tube for swallowing difficulties. At that time, CGH array analysis documented a deletion at 2q encompassing part of the *TTN* gene. A muscle biopsy was carried out showing variability in fibre size diameter, with the presence of some small and regular-shaped fibres. Hypospadias was detected with recurrent urinary tract infections during the follow-up. The

child was discharged at 3 months of life with the NG tube and O₂ support. In the following months, the child progressively improved until he no longer required respiratory support. He had some upper respiratory tract infections, but never had pneumonia.

Family H is characterised as a sporadic case with no family history of neuromuscular disease. The male proband presented at birth with bilateral clubfeet and generalised weakness. The pregnancy was otherwise normal with the exception of reduced fetal movement. Gross motor milestones were generally delayed, with walking attained at 19 months. The child had a clinical diagnosis of arthrogryposis multiplex congenita and underwent left quad-ricepsplasty during childhood to improve his gait as part of treatment for decreased joint mobility. Weakness and reduced muscle bulk in the lower limbs was noted, particularly of the left quadriceps as well as mild bilateral ptosis which together indicated an underlying neuromuscular disorder. Muscle biopsy of the left quadriceps before 10 years old was consistent with congenital fibre-type disproportion. Mobility in his knee, ankle, wrist, hip, jaw and shoulder joints has decreased with age. In late adolescence, he is fully ambulant and independent; however, he experiences muscle fatigue after long periods of standing. Weakness is predominantly proximal and more pronounced in the lower than the upper limbs. He has difficulty with raising his hands above his head as well as sitting on the floor due to shoulder and hip tightness. Pulmonary function is subnormal, but respiratory support is not required. Cardiac status was normal at last evaluation in early 10s.

Imaging data

In family A, muscle CT scan of II-3 was normal in the upper limbs, but showed bilateral and symmetrical atrophy of the rectus abdominis, semitendinosus, triceps sural and extensor digitorum of the toes.

CT scans of patient B-III-3 showed advanced fatty replacement of all lower limb, pelvic and paravertebral muscles with less severe degenerative changes in upper body parts.

In family D, imaging showed for patient D-I-2 severe fatty replacement of hamstrings and vastus lateralis in distal thigh, and of tibialis anterior and gastrocnemius in the lower legs; for patient D-II-1, early hypotrophy and fatty degeneration in adductor magnus and semimembranosus muscles of the thigh and asymmetric medial gastrocnemius, tibialis anterior and patchy soleus on the left lower leg; and for patient D-II-2, patchy fatty degeneration in the right soleus.

In patient E-III-1, MRIs identified severe fatty replacement in adductor longus and magnus, all hamstrings, rectus femoris and parts of vastus lateralis and intermedius of the thigh, total fatty replacement of tibialis anterior and right soleus on the lower legs with less changes in left soleus, right tibialis posterior and left extensor digitorum longus.

For patient G-II-1, MRIs showed severely hypotrophic gluteus maximus compared with medius and severe fatty involvement of pelvic obturators and less in adductor longus.

Molecular analysis

All CNVs are novel and not previously reported in the database of genomic variants (<http://dgv.tcag.ca/dgv/app/home>) except for families D and E. NGS analyses did not detect other *TTN* variants of interest, nor variants in other neuromuscular disease genes that might explain the patient's presentation.

Family A—Targeted NGS performed in patients II-2 and II-3 identified a heterozygous deletion encompassing exons 334–340. The boundaries of this deletion, defined by Sanger sequencing, are located within exons 334 and 340: chr2:g.179412605_179418808del; c.89030_93748del (figure 3A). This CNV results in truncation of part of exon 334 to part of exon 340 that predict an in-frame truncated transcript: c.89030_93748del without amino acid change at the junction and loss of 1573 amino acids (173 kDa), located in the A-band. RNAseq coverage analysis did not demonstrate nonsense-mediated mRNA decay (NMD) of transcripts carrying the CNV (approximately 50% of the reads) (figure 3A).

Family B—In this family, WES identified in affected patients II-1 and III-3 a heterozygous deletion with boundaries located by DNA genomic sequencing in introns 297 and 312:g.179448846_179459004del; c.58 151–35_65275+157 del. RNAseq analysis showed transcripts with deletion of exons 298–312, keeping an open reading frame. This CNV leads to the truncation of a part of the A-band, loss of 2375 amino acids (263 kDa). Read depth analysis of the RNAseq data did not suggest NMD of transcripts carrying the mutated allele (figure 3B).

Family C—The mother (I-1) and the two children (II-1 and II-3) have a heterozygous deletion from exon 94 to intron 128. Interestingly, the sequence breakpoints obtained by Sanger sequencing revealed the presence of identical sequences TTCA at the 3' and 5' junctions. The breakpoint sequences result in two possibilities: chr2:c.26786_c.32311+321 del or chr2:c.26783_c.32311+317 del, leading in both cases to deletion of the donor splice site of exon 94 that predicts exon 94 skipping from the transcripts. Unfortunately, due to the lack of patient muscle biopsy, RNA analysis was not possible to evaluate whether activation of a cryptic donor splice site occurred. If we consider the hypothesis of a deletion of exons 94–128, the reading frame would be preserved and the CNV would result in a deletion localised in the titin I-band which partially truncates the PEVK domain. The predicted protein translated would have a loss of 1850 amino acids (207 kDa). In this family, patient II-3 is also affected by SMA due to biallelic exon 7 deletion of the *SMN1* gene, with three copies of this exon in the *SMN2* gene.

Families D–E—NGS analyses identified in families D and E a heterozygous deletion of *TTN* exons 11–18, with breakpoints in intron 10 and 18 determined by Sanger sequencing to be very close to exon–intron junctions, chr2:c.1662+15_3101-3del, resulting in 16 nucleotides long recombinant intron between exons 10 and 19.⁶ RNAseq analysis confirmed the retention of the 16-nucleotide recombinant intron in the mutant allele (figure 3C). The sequencing depth of intron retention showed a proportion of deleted transcripts close to 50%, suggesting that NMD of the deleted allele is probably absent or minimal.⁶ The predicted protein translated would be 60 kDa (figure 3C).

Family F—CGH array analysis identified a de novo heterozygous intragenic *TTN* deletion. A trio NGS analysis confirmed the deletion on the maternal allele and refined the breakpoints in intron 295 and in exon 327 (chr2:179434372_179462179del). RNAseq analysis indicated the presence of two populations of aberrant transcripts in phase: a major one with deletion of exons 296–327, resulting in a loss of 9759 amino acids (1077 kDa) (NM_001267550.1:r.57545_86821del p.(Asp19182_Thr28940del)), and a minor one with a deletion of exons 295–327 (figure 3D). NMD of the deleted allele is probably absent or minimal, as indicated by balanced allelic ratios for 10 phased SNPs (data not shown).

Family G—CGH array analysis identified a large de novo heterozygous intragenic *TTN* deletion. Sequencing analysis confirmed the heterozygous deletion and mapped the breakpoints in intron 47 and intron 220 (chr2:g.179506480_179617668del).

RNAseq analysis indicated the presence of a transcript with the deletion of exons 48–220, resulting in a loss of 8426 amino acids (934 kDa) (NM_001267550.1: r.11312_40558del p.(Glu3771_Ser13519del) (figure 3E). Based on allelic ratio for five SNPs, NMD of the deleted allele is probably absent or minimal (data not shown).

Family H—Read depth analysis of an NGS 43-gene sequencing panel identified a large heterozygous intragenic deletion of the *TTNI*-band. Trio ddPCR of sequences within exon 55 confirmed the heterozygous deletion as de novo. Long-read PacBio sequencing confirmed a 119 383 bp deletion (chr2:g.179517492–179636871) encompassing exons 34–200. RNAseq analysis of gastrocnemius mRNA revealed a prominent abnormal splice variant predicting production of an internally deleted in-frame protein lacking exons 34–200 from roughly half the sequenced transcripts and loss of 8918 amino acids (990 kDa) (figure 3F).

DISCUSSION

Here, we demonstrate phenotypical diversity among dominant titinopathies resulting from intragenic CNV deletions of the *TTN* gene. Location in the gene and size of the deletions are variable and there is evident clinical heterogeneity between families but with a predominance of distal involvement in five families of our cohort (figure 4). It is interesting to note that affected members of three families, C, G and H, in whom arthrogryposis is a prominent feature of the disease, all had deletions involving the Ig-like domains of the I-band including the metatranscript-only exons (exons not included in any of the cardiac and skeletal muscle isoforms). More cases will be needed to be identified in order to determine whether these preliminary observations hold as reliable genotype–phenotype associations.

In two of our families, some patients had additional abnormalities. In family B, although both patients (II-1 and his son III-3) share a prominent distal muscle involvement, patient III-3, in whom moderate dystrophin abnormalities were identified, also has proximal muscle weakness and DCM. However, no mutation was detected in the *DMD* gene nor transcripts, nor in genetic coding for proteins that interact directly with dystrophin. A secondary dystrophin defect due to CNV *TTN* is unlikely since the father (II-1) does not have a

dystrophin defect. This defect could be due to a *DMD* variant not identified with the techniques used, or be secondary to another genetic defect.

In family C, patient II-3 was first diagnosed as SMA-II with homozygous *SMN1* deletion. This patient then developed diffuse joint contractures (elbows, wrists, fingers, ankles) that were considered as unusual for typical SMA-II and lead to genetic reanalysis that revealed the *TTNCNV* deletion. Similarly, his older brother (II-1) as well as mother (I-2) developed also joint contractures. The latter two carried the *TTNCNV* deletion but not the homozygous *SMN1* deletion. Although we cannot rule out a gene interaction, the most likely mechanism is the addition of the phenotypes of the two pathologies in the patient, with the delayed motor milestones due to *SMN1* mutation and the diffuse joint contractures caused by the *TTNCNV* deletion.

The diagnosis yield of NGS for primary myopathies varies between 30% and 50%.¹⁷ Efficient detection of CNVs is a major challenge for improving the diagnostic rate in rare neuromuscular diseases, even more in the *TTN* gene which is characterised by the presence of three repeated regions (for which the relative quantification lacks reliability). Due to the complex nature of *TTN* gene, several orthogonal approaches are recommended be used.¹⁸⁻²¹ Improved detection combined with an increase in the number of CNVs in genetic databases could promote better understanding of new genotype–phenotype associations. Long-read DNA, whole-genome and RNA sequencing approaches, as well as optical genomic mapping performed in a more routine manner should help to identify CNV rearrangements.²² Concerning the mechanisms of these large rearrangements, identification in family C of identical sequences TTCA at 3' and 5' junctions suggests a non-homologous joining event as they frequently occur at microhomology sites.²³

The RNAseq approach is very useful to define the transcripts resulting from the identified CNV. We used polyA or ribodepletion to analyse muscle transcripts. PolyA capture of transcripts is limited by less efficient capture and therefore less sequencing coverage of the 5' parts of very large transcripts such as for titin. Ribodepletion significantly enriches for mRNA, and thus has very high sensitivity, with the disadvantage of a high background of aberrant transcripts. In this cohort, the reading frame was maintained in transcripts for families A, B, F, G and H but not for families D and E. The reading frame of resulting transcripts in family C could not be determined in the absence of available muscle for RNAseq analyses.

Since haploinsufficiency is not a reasonable pathomechanism considering the high frequency of titin truncating variants in the general population, we believe that the dominant effect of the in-phase deleted CNVs could be due to a recombinant protein with aberrant domain alignment that would alter its conformation. It would lead to aberrant protein interactions (toxic gain-of-function effect) and/or interact with the wild-type titin to inhibit its normal function (dominant-negative effect).⁶ This mechanism would require that a stable truncated protein is produced. NMD mechanism of mutated transcripts appeared to be absent or minimal in these families, whether the phase is maintained or not. For families A, B, F, G and H, in the absence of a predicted premature stop codon and of NMD, we can assume the translation of internally deleted proteins (but due to the priority for RNA analysis, western

blot analyses were not performed). Similar mechanisms can be suggested with another giant protein, nebulin, where a truncated protein is detected as a result of large dominant deletions in the *NEB* gene.^{24 25} In families D and E, the deletion of exons 11–18 results in the loss of the reading frame due to partial intronic retention of introns 10 and 18 and thereby a premature stop codon. In the absence of detectable NMD, the deletion is predicted to lead to a titin protein of 60 kDa lacking a large part of the I-band, all A-band and M-band. The predicted truncated protein would preserve the insertion domains in the Z-disk, suggesting a possible dominant-negative effect. However, western blot analyses with current techniques did not detect any truncated protein.⁶

Peculiarly, the phenotype has an adult onset and a clear distal component (figure 4). The best known dominant titinopathies with distal preference are missense variants in exon 364 causing late-onset tibial muscular dystrophy²⁶ and some of the known missenses in exon 344 causing hereditary myopathy with early respiratory failure.²⁷ In our series of dominant deletions, the phenotype surprisingly often had a distal presentation irrespective of deletion position which may be compatible with the alternative of the mutant harming the wild-type protein.

Titin interacts with a large number of proteins²⁸ and these interactions are essential for proper muscle structure and function. Some of these interactions are essential for cell signalling,^{29 30} others for an elasticity component³¹ or in the transduction of the mechanical signal, in particular by its interactions with myosin and actin.^{23 31} The diversity of CNVs in our cohort suggests that different interaction domains may be affected when truncated titin proteins are integrated into the sarcomere. The integration of these proteins could destabilise the titin-dependent protein network. For families A, B and F, the CNVs affect different myosin interaction domains in the A-band (exons 334–340 and exons 297–313, 296–327). For families G and H, the deletion is very large, removing domains going from I-band to A-band (the actin interaction domains, the PEVK and part of the myosin interaction domains). Recent genotype–phenotype association studies have shown that variants affecting the PEVK domain were associated with arthrogryposis-like phenotypes as in families G and H,^{32–38} which can be understood as a consequence of amyoplasia caused by mutated metatranscript exons with preferential fetal expression.

The presence of cardiomyopathy in some but not all patients in this study is of interest. When the deletion co-segregates with cardiomyopathy, the most likely explanation is that it affects isoforms important for cardiac muscle. In families without complete co-segregation, we postulate the involvement of a modifying gene or a second mutated gene (digenism).

Animal and cellular models would be useful to evaluate the presence, location and behaviour of the deleted protein and to advance in the understanding of the pathogenic dominant mechanisms of *TTN* CNV and genotype–phenotype associations. Also, the finding of smaller deletions being able to cause a distal phenotype changes the diagnostic approach in patients with a distal myopathy as CNVs need to be considered in addition to pathogenic variants in the C-terminal *TTN* exons and in the already known other genes.

Supplementary Material

Refer to Web version on PubMed Central for supplementary material.

Acknowledgements

The authors thank AFM-Telethon for their financial support, French titin consortium for their discussion about patients, and Heng Li, Jason Chin, Joseph Devaney and the team at GeneDx for long-range sequencing and interpretation of data for family H. In particular, heartfelt thanks to all the patients and their families for their participation without which these research studies would not have been possible.

Funding

This work was funded by AFM 21381 and 24259 grants (the French Muscular Dystrophy Association (AFM-Téléthon)); the Délégation à la Recherche Clinique et à l'Innovation du Groupement de Coopération Sanitaire de la Mission d'Enseignement, de Recherche, de Référence et d'Innovation (DRCI-GCS-MERRI) de Montpellier-Nîmes and the Solve-RD Project have received funding from the European Union's Horizon 2020 research and innovation programme under grant agreement no 779257. Analysis of family H was supported by Muscular Dystrophy Association (USA) grant MDA602235, Boston Children's Hospital IDDRC Molecular Genetics Core Facility funded by P50HD105351 from the National Institutes of Health of USA, the Boston Children's Hospital CRDC Initiative and by a sponsored research agreement with GeneDx. Some coauthors are members of the ERN NMD Network (AD'A, FF, OB-T, MS, RBY, IN, GS, YP, ESB, AS, MJ, BU, GB).

Data availability statement

All data relevant to the study are included in the article or uploaded as supplemental information.

REFERENCES

1. Linke WA, Hamdani N. Gigantic business: Titin properties and function through thick and thin. *Circ Res* 2014;114:1052–68. [PubMed: 24625729]
2. Savarese M, Maggi L, Vihola A, et al. Interpreting genetic variants in Titin in patients with muscle disorders. *JAMA Neurol* 2018;75:557–65. [PubMed: 29435569]
3. Savarese M, Sarparanta J, Vihola A, et al. Increasing role of Titin mutations in neuromuscular disorders. *J Neuromuscul Dis* 2016;3:293–308. [PubMed: 27854229]
4. Välipakka S, Savarese M, Johari M, et al. Copy number variation analysis increases the diagnostic yield of NGS studies in muscle disease patients. *Neuromuscular Disorders* 2017;27:S193–4.
5. Roggenbuck J, Rich K, Morales A, et al. A novel TTN deletion in a family with skeletal myopathy, facial weakness, and dilated cardiomyopathy. *Mol Genet Genomic Med* 2019;7:e924. [PubMed: 31489791]
6. Perrin A, Juntas Morales R, Chapon F, et al. Novel dominant distal titinopathy phenotype associated with copy number variation. *Ann Clin Transl Neurol* 2021;8:1906–12. [PubMed: 34312993]
7. Sagath L, Lehtokari V-L, Välipakka S, et al. An extended targeted copy number variation detection array including 187 genes for the diagnostics of neuromuscular disorders. *J Neuromuscul Dis* 2018;5:307–14. [PubMed: 30040739]
8. Välipakka S, Savarese M, Sagath L, et al. Improving copy number variant detection from sequencing data with a combination of programs and a predictive model. *J Mol Diagn* 2020;22:40–9. [PubMed: 31733349]
9. Zenagui R, Lacourt D, Pegeot H, et al. A reliable targeted next-generation sequencing strategy for diagnosis of myopathies and muscular dystrophies, especially for the giant Titin and Nebulin genes. *J Mol Diagn* 2018;20:533–49. [PubMed: 29792937]
10. Evilä A, Arumilli M, Udd B, et al. Targeted next-generation sequencing assay for detection of mutations in primary myopathies. *Neuromuscul Disord* 2016;26:7–15. [PubMed: 26627873]

11. Marttila M, Win W, Al-Ghamdi F, et al. Myl2-associated congenital fiber-type disproportion and cardiomyopathy with variants in additional neuromuscular disease genes; the dilemma of panel testing. *Cold Spring Harb Mol Case Stud* 2019;5:a004184. [PubMed: 31127036]
12. Rockowitz S, LeCompte N, Carmack M, et al. Children's rare disease cohorts: an integrative research and clinical genomics initiative. *NPJ Genom Med* 2020;5:29. [PubMed: 32655885]
13. Perrin A, Juntas Morales R, Rivier F, et al. The importance of an integrated genotype-phenotype strategy to unravel the molecular bases of titinopathies. *Neuromuscul Disord* 2020;30:877–87. [PubMed: 33127292]
14. Dobin A, Davis CA, Schlesinger F, et al. STAR: ultrafast universal RNA-Seq Aligner. *Bioinformatics* 2013;29:15–21. [PubMed: 23104886]
15. Thorvaldsdóttir H, Robinson JT, Mesirov JP. Integrative Genomics viewer (IGV): high-performance genomics data visualization and exploration. *Brief Bioinform* 2013;14:178–92. [PubMed: 22517427]
16. Garrido-Martín D, Palumbo E, Guigó R, et al. Ggsashimi: Sashimi plot revised for browser- and annotation-independent splicing visualization. *PLoS Comput Biol* 2018;14:e1006360. [PubMed: 30118475]
17. Juntas Morales R, Perrin A, Solé G, et al. An integrated clinical-biological approach to identify Interindividual variability and atypical phenotype-genotype correlations in myopathies: experience on A cohort of 156 families. *Genes (Basel)* 2021;12:1199. [PubMed: 34440373]
18. Demidov G, Sturm M, Ossowski S. ClinCNV: multi-sample germline CNV detection in NGS data. *Bioinformatics* [Preprint] 2022.
19. Fawcett KA, Demidov G, Shrine N, et al. Exome-wide analysis of copy number variation shows Association of the human Leukocyte antigen region with asthma in UK Biobank. *BMC Med Genomics* 2022;15:119. [PubMed: 35597955]
20. Plagnol V, Curtis J, Epstein M, et al. A robust model for read count data in exome sequencing experiments and implications for copy number variant calling. *Bioinformatics* 2012;28:2747–54. [PubMed: 22942019]
21. Chen X, Schulz-Trieglaff O, Shaw R, et al. Manta: rapid detection of structural variants and Indels for Germline and cancer sequencing applications. *Bioinformatics* 2016;32:1220–2. [PubMed: 26647377]
22. Mantere T, Neveling K, Pebrel-Richard C, et al. Optical genome mapping enables constitutional chromosomal aberration detection. *Am J Hum Genet* 2021;108:1409–22. [PubMed: 34237280]
23. Luis NM, Schnorrer F. Mechanobiology of muscle and myofibril Morphogenesis. *Cells Dev* 2021;168:203760. [PubMed: 34863916]
24. Sagath L, Lehtokari V-L, Välipakka S, et al. Congenital asymmetric distal myopathy with hemifacial weakness caused by a heterozygous large de novo mosaic deletion in Nebulin. *Neuromuscul Disord* 2021;31:539–45. [PubMed: 33933294]
25. Kiiski KJ, Lehtokari V-L, Vihola AK, et al. Dominantly inherited distal Nemaline/cap myopathy caused by a large deletion in the Nebulin gene. *Neuromuscul Disord* 2019;29:97–107. [PubMed: 30679003]
26. Hackman P, Vihola A, Haravuori H, et al. Tibial muscular dystrophy is a titinopathy caused by mutations in TTN, the gene encoding the giant skeletal-muscle protein Titin. *Am J Hum Genet* 2002;71:492–500. [PubMed: 12145747]
27. Palmio J, Leonard-Louis S, Sacconi S, et al. Expanding the importance of HMERF titinopathy: new mutations and clinical aspects. *J Neurol* 2019;266:680–90. [PubMed: 30666435]
28. Kontogianni-Konstantopoulos A, Ackermann MA, Bowman AL, et al. Muscle giants: molecular scaffolds in sarcomerogenesis. *Physiol Rev* 2009;89:1217–67. [PubMed: 19789381]
29. Lange S, Xiang F, Yakovenko A, et al. Cell biology: the kinase domain of Titin controls muscle gene expression and protein turnover. *Science* 2005;308:1599–603. [PubMed: 15802564]
30. Lange S, Pinotsis N, Agarkova I, et al. The M-band: the underestimated part of the sarcomere. *Biochim Biophys Acta Mol Cell Res* 2020;1867:118440. [PubMed: 30738787]
31. Linke WA. Titin gene and protein functions in passive and active muscle. *Annu Rev Physiol* 2018;80:389–411. [PubMed: 29131758]

32. Averdunk L, Donkervoort S, Horn D, et al. Recognizable pattern of arthrogryposis and congenital myopathy caused by the recurrent TTN metatranscript-only C.39974-11T>G splice variant. *Neuropediatrics* 2022;53:309–20. [PubMed: 35605965]
33. McDermott H, Henderson A, Robinson HK, et al. Novel compound heterozygous TTN variants as a cause of severe neonatal congenital contracture syndrome without cardiac involvement diagnosed with rapid trio Exome sequencing. *Neuromuscul Disord* 2021;31:783–7. [PubMed: 34303570]
34. Savarese M, Vihola A, Oates EC, et al. Genotype–phenotype correlations in recessive titinopathies. *Genet Med* 2020;22:2029–40. [PubMed: 32778822]
35. Bryen SJ, Ewans LJ, Pinner J, et al. Recurrent TTN metatranscript-only C.39974–11T>G splice variant associated with autosomal recessive arthrogryposis multiplex congenita and myopathy. *Hum Mutat* 2020;41:403–11. [PubMed: 31660661]
36. Fernández-Marmiesse A, Carrascosa-Romero MC, Alfaro Ponce B, et al. Homozygous truncating mutation in prenatally expressed skeletal isoform of TTN gene results in arthrogryposis multiplex congenita and myopathy without cardiac involvement. *Neuromuscul Disord* 2017;27:188–92. [PubMed: 28040389]
37. Oates EC, Jones KJ, Donkervoort S, et al. Congenital titinopathy: comprehensive characterization and pathogenic insights. *Ann Neurol* 2018;83:1105–24. [PubMed: 29691892]
38. Di Feo MF, Lillback V, Jokela M, et al. The crucial role of Titin in fetal development: recurrent miscarriages and bone, heart and muscle anomalies characterise the severe end of Titinopathies spectrum. *J Med Genet* 2023;60:866–73. [PubMed: 36977548]
39. Xie Y, Li H, Luo X, et al. IBS 2.0: an upgraded illustrator for the visualization of biological sequences. *Nucleic Acids Res* 2022;50:W420–6. [PubMed: 35580044]

WHAT IS ALREADY KNOWN ON THIS TOPIC

- Titinopathies are complex neuromuscular disorders, with a great diversity of phenotypes and autosomal recessive or dominant inheritance. Most pathogenic variants are single nucleotide variant; only few deletion-type CNVs have been reported so far, in scarce case reports and without clear genotype–phenotype associations.

WHAT THIS STUDY ADDS

- This is the first publication of a rather large series of patients (n=17) with titinopathies due to dominant CNVs in the *TTN* gene, in whom we have performed a deep phenotyping and molecular characterisation.

HOW THIS STUDY MIGHT AFFECT RESEARCH, PRACTICE OR POLICY

- The finding of *TTN* deletions being able to cause dominant disease and even later-onset distal phenotype changes the diagnostic approach in patients with a distal myopathy as CNVs need to be searched in addition to pathogenic variants in the C-terminal *TTN* exons and in the known other genes.

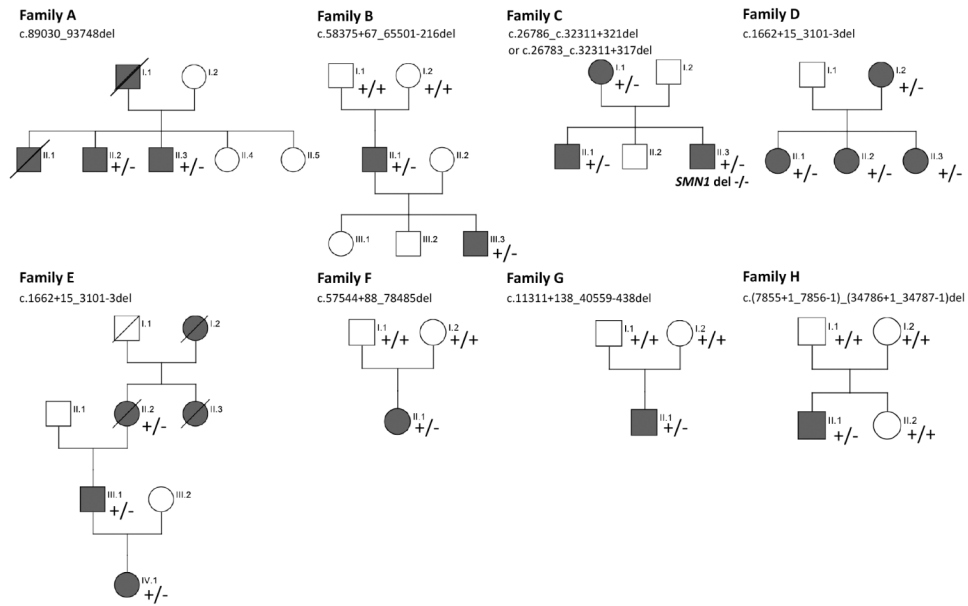


Figure 1. Patients' family pedigrees. Family members with a pathological phenotype are reported in black. Deceased individuals are crossed out. Genotypes are reported as $+/+$ for wild-type (absence of the deletion) and $+/-$ for heterozygous deletion. For each family, the identified *TTN* deletion is reported under the family name.

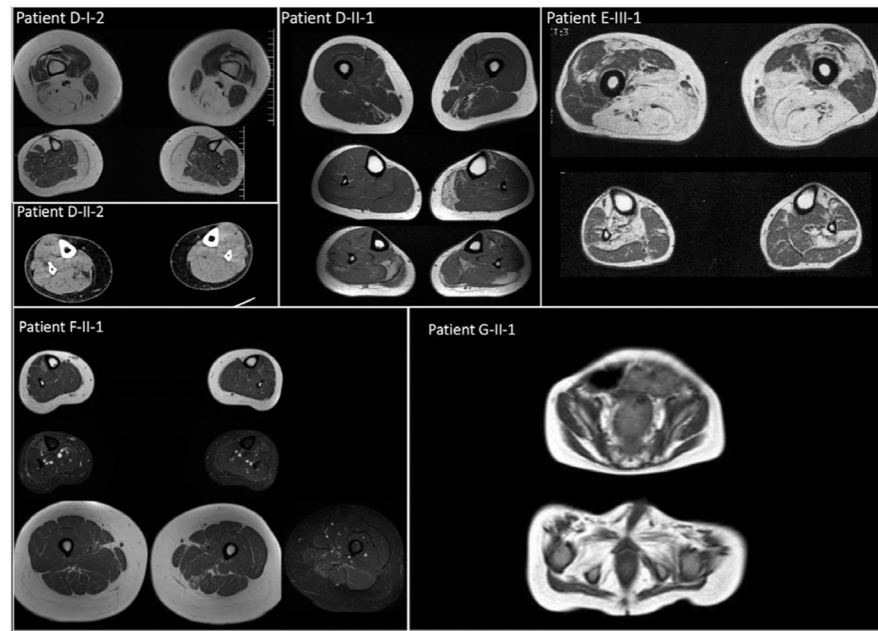


Figure 2.

Muscle MRIs. Muscle MRI of D-I-2 shows severe fatty replacement in adductor magnus and hamstrings as well as total replacement of tibialis anterior and medial gastrocnemius. CT scan of D-II-2 shows focal fatty changes in the right medial gastrocnemius and tibialis anterior. MRIs of D-II-1 show mild focal fatty involvement of both semimembranosus and adductor magnus on the left side together with focal changes in the left tibialis anterior, medial and lateral gastrocnemius and soleus and soleus on the right leg. MRIs of E-III-1 display extensive fatty replacement in all hamstrings, adductor muscles and rectus femoris with less involvement of vastus lateralis and intermedius. On the lower legs, fatty dystrophic change is present in tibialis anterior and soleus, less on the left side. MRIs of F-II-1 do not reveal dystrophic changes but degenerative change in the left semimembranosus with mild oedema on short tau inversion recovery sequences. In G-II-1, there is a different pattern of changes with high degree of atrophy in gluteus maximus and fatty involvement of obturatorius muscles.

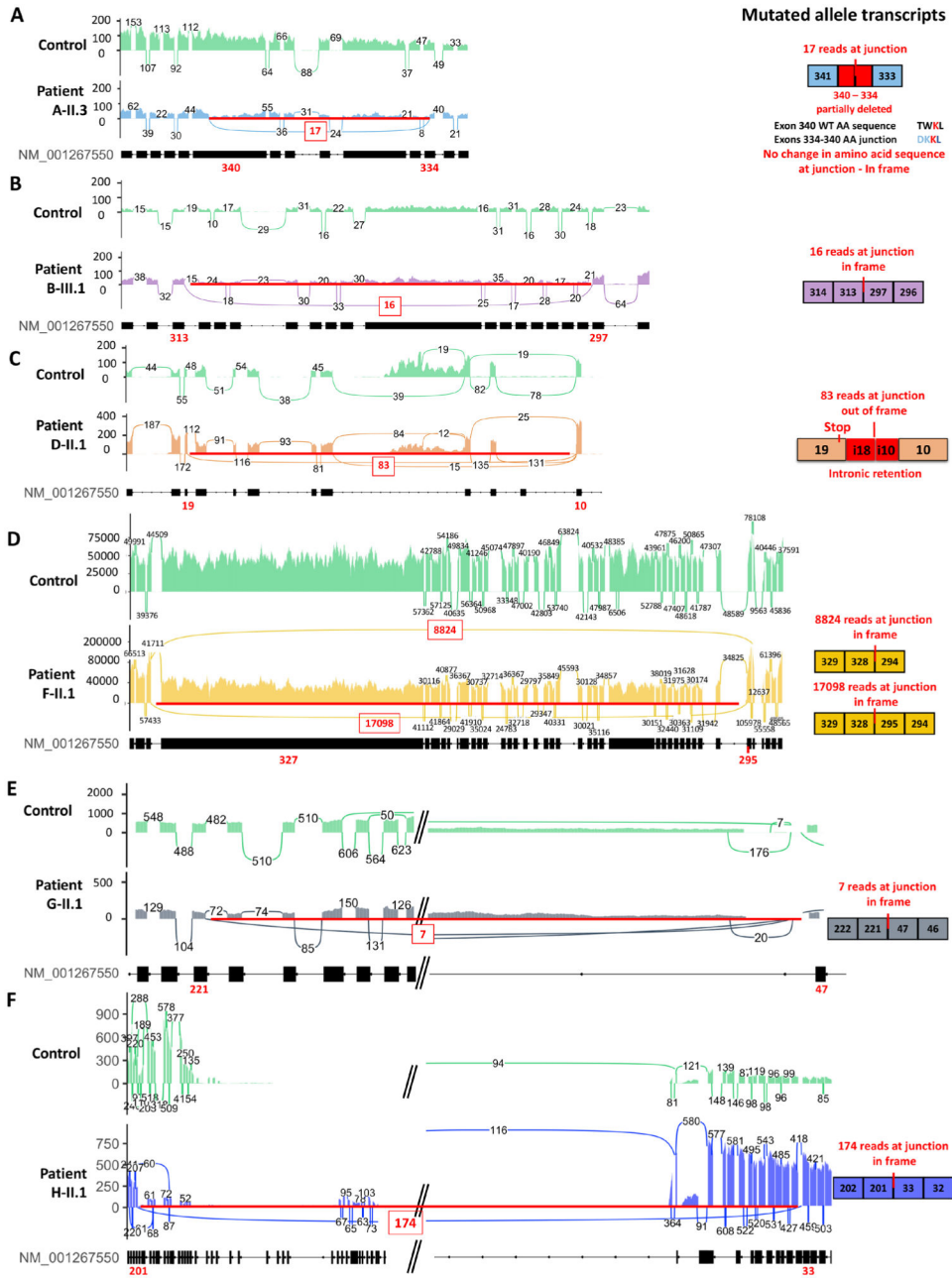


Figure 3. RNA sequencing (RNAseq) analyses. Analysis of RNAseq data of muscle biopsy from patients for whom a biopsy was available and from a healthy control (in green). The red bar for each patient sashimi plot represents the genomic location of CNVs. The numbers associated with each junction arc represent the number of reads that contain exon/exon junctions. The number of reads of newly created junctions is noted in red boxes. On the right panel, representation of deleted mRNA alleles is shown. Abnormal junctions resulting from CNVs in each patient are indicated by a red line. (A) Blue is patient II.3 of family A for which the consequences at the mRNA level are associated, that is, the creation of a new in-frame junction with a partial deletion of exons 334 and 340. (B) Purple is patient III-1

of family B for which the consequence of CNV is the creation of an in-frame junction of exons 297 and 313. (C) Orange is patient II-1 of family D for which the CNV will induce the intronic out-of-frame retention of 2 nucleotides of intron 18 and 14 nucleotides of intron 10. (D) Patient F-II-1 for which the CNV induces two significant in-phase mRNA deleted alleles. (E) Patient G-II-1 with newly junction from exon 47 to exon 221. (F) Patient H-II-1 with a deletion of exons 34–200 (red line) and a new junction created between exons 34 and 201.

Author Manuscript

Author Manuscript

Author Manuscript

Author Manuscript

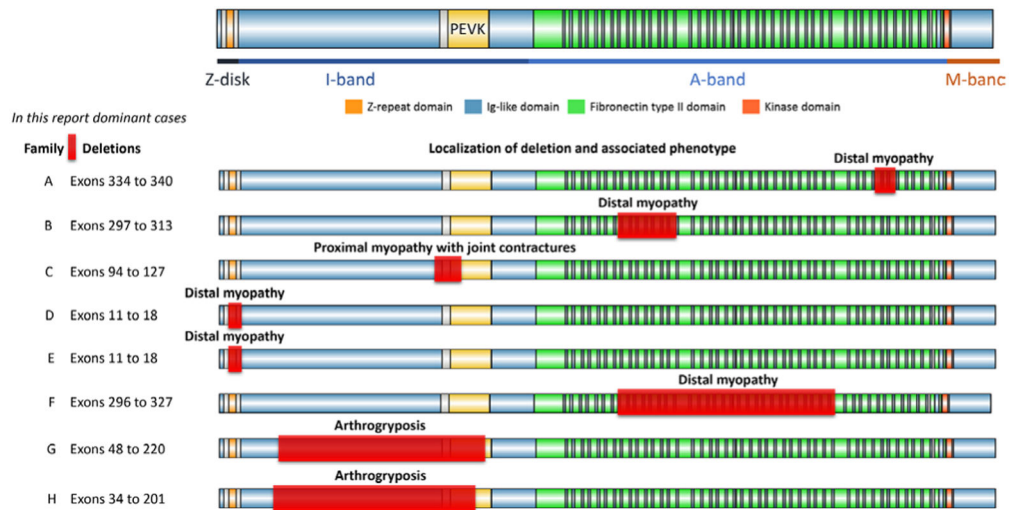


Figure 4. Location of CNVs and associated skeletal muscle phenotype. Deletions are represented with a red bar and associated phenotypes are mentioned above the deletion location. The deletion identified in families D and E was out-of-frame. Other deletions were in-frame or suspected to be in-frame (family C) (figure was designed with IBS³⁹).